research papers

Versatile vacuum chamber for *in situ* surface X-ray scattering studies

**Dina Carbone,[a]* Olivier Plantevin,[a,b] Raul Gago,[c] Cristian Mocuta,[a]
Oier Bikondoa,[a] Alejandro Alija,[a,d] Lucien Petit,[a] Hamid Djazuli[a] and
Till-Hartmut Metzger[a]**

[a]ID01, ESRF, Grenoble, France, [b]Centre de Spectrométrie Nucleaire et de Spectrometrie de Masse,
Orsay, France, [c]Centro de Micro-Análisis de Materiales, Universidad Autónoma de Madrid, Spain,
and [d]Universidad de Oviedo, Spain. E-mail: gcarbone@esrf.fr

A compact portable vacuum-compatible chamber designed for surface X-ray
scattering measurements on beamline ID01 of the European Synchrotron
Radiation Facility, Grenoble, is described. The chamber is versatile and can be
used for *in situ* investigation of various systems, such as surfaces, nanostructures,
thin films *etc.*, using a variety of X-ray-based techniques such as reflectivity,
grazing-incidence small-angle scattering and diffraction. It has been conceived
for the study of morphology and structure of semiconductor surfaces during ion
beam erosion, but it is also used for the study of surface oxidation or thin film
growth under ultra-high-vacuum conditions. Coherent X-ray beam experiments
are also possible. The chamber is described in detail, and examples of its use
are given.

1. Introduction

Surface-sensitive X-ray scattering techniques such as grazing-incidence small-angle X-ray scattering (GISAXS) and grazing-incidence diffraction (GID) are widely used to investigate structure and morphology of surfaces and near-surface layers (Stangl *et al.*, 2000). Typical examples include absorption (Ackermann *et al.*, 2005), reconstruction (Joumard *et al.*, 2006), thin films (Pietsch *et al.*, 2004) and mesoscopic structures (Schmidbauer, 2004). These characterization methods can also be used to follow the growth or the evolution of the surfaces *in situ* (Valvidares *et al.*, 2004), and this requires the use of an appropriate sample environment. Often surface studies demand ultra-high-vacuum (UHV) conditions, for example, to avoid contamination. There are several examples of UHV chambers designed for this purpose (Nicklin *et al.*, 1998; Bernard *et al.*, 1999). Examples of chambers designed for high-pressure studies can also be found in the literature (Bernard *et al.*, 1999).

Here we present a compact vacuum-compatible chamber designed for *in situ* X-ray scattering studies over a wide pressure range, bridging the ambient pressure and the UHV regime. Originally it was conceived for the study of nanostructure formation on semiconductor surfaces by ion beam sputtering (IBS). IBS in the low-energy range (E = 0.1–10 keV) is a technique recently exploited for the self-organized production of ordered uniform structures on the surface of different materials like semiconductors (*e.g.* Si, GaSb), metals and insulators, with size down to 10 nm (Valbusa *et al.*,

2002; Facsko *et al.*, 1999; Ziberi *et al.*, 2005; Gago *et al.*, 2001). The use of *in situ* X-ray scattering to study the formation and stabilization of the different nanostructures *during* the sputtering process is an innovative approach to understanding the IBS process. Structural characterization of the nanopatterned surfaces is generally carried out by use of *ex situ* imaging techniques (such as atomic force microscopy or transmission electron microscopy) after the ion erosion process. Our approach combines the characteristics of non-destructiveness and high statistical sampling typical of X-rays with the capability of performing *real-time* studies, with a resolution of a few seconds not achievable by *ex situ* techniques.

The chamber is optimized to work at a medium-range pressure (10^{-3}–10^{-7} mbar). However, with small modifications of its configuration and with appropriate preparation (*i.e.* long baking, use of UHV-compatible components *etc.*), the base pressure can be lowered in the 10^{-10} mbar regime and the chamber can easily be used for UHV experiments. We describe the design of the chamber and its use on the diffractometer for *in situ* studies, or off-line for preparation/optimization of the samples and experimental conditions. Making use of the modularity of the chamber's components and the different arrangements of the ports, the chamber can be used for various kinds of experiments.

2. Description

The compact design of the chamber, shown in Fig. 1, allows the use of different scattering geometries and experimental set-
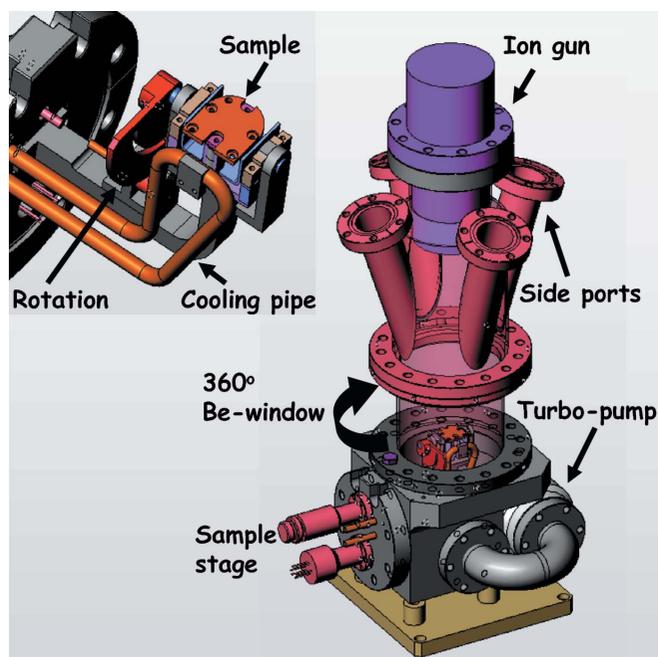
Figure 1
Schematics of the portable chamber. See text for details. Inset: manipulator for IBS experiments. Sample rotation and cooling pipe are indicated.

ups. The chamber has a stainless steel body; it is about 56 cm in height, has a volume of ~ 3 l and weighs around 12 kg. The lower part of the body has two CF38 and one CF63 flanges, the latter being used to introduce the sample holder. The central part of the chamber consists of a 2 mm-thick cylindrical Be window that surrounds the sample. This window, with acceptance angles of 360° and 40° in the horizontal and vertical direction, respectively, allows for flexible scattering geometries using X-rays in the hard X-ray regime.[1] Four removable support rods secure the Be window during transport or mounting/dismounting of the chamber. During the X-ray scattering experiments, these rods can be put in different positions around the Be window to avoid shadowing that would result in inaccessible areas in angular space. The top part of the chamber presents one US $4\frac{5}{8}''$ flange foreseen for the ion gun mount. Four more CF38 flanges are used for introducing other equipment, such as evaporation sources, gas inlets, vacuum gauges, viewports *etc.*

The vacuum is provided by a turbo-molecular pump (Varian V70-LP2) with a pumping speed of ~ 45 l s^{-1}. A Leybold Inficon (IR090) pressure gauge, using a hot cathode and a Pirani system, reads the pressure in the range 10^{-10}–10^3 mbar.

2.1. Ion beam sputtering configuration

For the study of semiconductor surface modification during IBS, the chamber is equipped with a 3 cm-diameter Kaufman ion source (Veeco Instruments). Mounted on the top flange of the chamber, it delivers ion current densities up to 1 mA cm^{-2} in the energy range 100–1200 eV using different gases (Ar,

Xe, Kr). A collimating graphite double-grid set reduces the divergence of the ion beam down to a minimum of $\sim 10°$.

One of the main characteristics of IBS on semiconductor surfaces is the dependence of nanostructure morphologies and lateral order on the angle of incidence of the ion beam (Facsko *et al.*, 1999; Ziberi *et al.*, 2005). Therefore, a fundamental aspect of the set-up for this type of *in situ* study is the capability of orienting the sample surface with respect to the direction of incidence of both the ion beam *and* the X-ray beam. For this purpose, a special sample holder has been designed, which allows the rotation of the sample surface with respect to the ion gun over a wide angular range (0°–90°) with $\pm 0.7°$ accuracy, while keeping the sample in the centre of the chamber (therefore in the centre of rotation of the diffractometer), at ~ 10 cm from the ion source. Further adjustments of the sample with respect to the X-ray beam can be carried out using the tilt angles of the diffractometer, as described in more detail in §3.

A schematic diagram of the sample holder is shown in the inset of Fig. 1. The manipulator flange has feedthroughs for a set of cooling pipes, two sets of electrical connections for the heater and the thermocouple cables. The cooling system, necessary to dissipate the heat produced on the sample during IBS, owing to the large current delivered by the ion gun, uses chilled water (60% water and 40% glycerol) at a base temperature $T = 253$ K. The thermal contact between the rigid cooling pipe and the sample holder is assured by a flexible copper braid. A commercially available ceramic heating plate allows the control of the substrate temperature with ± 1 K accuracy in the range between room temperature and ~ 1000 K. The base pressure achievable in this configuration is 10^{-7} mbar.

Recent publications based on the use of this chamber are by Plantevin *et al.* (2007) and Carbone *et al.* (2008).

2.2. UHV surface diffraction configuration

The configuration of the chamber can be modified for thin film growth and other surface-sensitive studies requiring UHV (*e.g.* studies of surfaces and interfaces in a controlled atmosphere). With proper cleaning of the components and bake-out of the chamber, pressure in the low 10^{-9}–10^{-10} mbar regime can be achieved, even without the use of an ion pump (this is mostly due to the small volume of the chamber). Still, a small ion pump can be placed on one of the free lateral ports, if needed. The main modification to the set-up of the chamber is the re-location of the turbo pump, that replaces the Veeco ion gun on the top of the chamber. Side ports are then used for evaporation sources, gas inlets, ion sputter gun for cleaning surfaces *etc.* The chamber can be used to prepare samples off-line prior to the X-ray experiments. Afterwards, using a portable power supply, the chamber can be brought from the preparation laboratory to the diffractometer without switching off the electric equipment, therefore preserving the optimized conditions for the experiment.

For thin film deposition, an electron bombarded evaporation source (Omicron EFM-3 or EFM-4) can be mounted on

---

[1] The transmission through this window falls below 50% for X-ray energies lower than 7 keV, and it is higher than 80% above 10 keV.

one of the side ports on the top of the chamber. The source material is shaped as a rod of diameter 2 mm and up to 50 mm in length that can be translated within the evaporation device such that the electron beam impinges on one end and evaporates the material locally. This allows the source to be used in different geometries including the vertical case.[2] The distance between source and substrate is about 15 cm. It allows the deposition of a wide range of materials,[3] *e.g.* metals and semiconductors, with typical deposition rates in the range 0.1–1 Å min^{-1}. Such a low evaporation rate makes the *in situ* studies easily feasible, during the growth process. The use of multi-target evaporation sources, or separate sources on different ports, allows the growth of layered or composite systems. A standard Ar$^+$ sputter gun for cleaning surfaces is also available. Thin film growth can be carried out in a controlled atmosphere (Ar, O_2 or gas mixtures); the simultaneous use of two gases is possible.

The ceramic sample holder used in this configuration has a similar design as the one described in Fig. 1, without the rotation stage for better mechanical stability. This allows a better control of the sample alignment with respect to the incident X-ray beam, necessary for surface diffraction in grazing-incidence geometry where sample rotation over large azimuth angles is required. As in the previous case, a ceramic heating plate is available for *in situ* UHV studies in the temperature range from room temperature to ~1000 K.

2.3. Coherent X-ray scattering

The chamber has also been implemented for coherent X-ray scattering experiments. For this purpose, it must preserve as much as possible the coherence properties of the X-ray beam. In our case, the 360° beryllium window, machined and non-polished, is inadequate because, owing to its micro-crystallinity and roughness of the order of several micrometres, spurious speckles are produced when using a coherent beam. This is illustrated in Fig. 2, where an example of a coherent diffraction experiment from a set of narrow slits is shown. For these measurements we used a set of polished cylindrical blades (Le Bolloc'h *et al.*, 2002), with 2 µm aperture and an X-ray beam energy of 8 keV. Measurements were performed in the horizontal plane. The distance between the slits and detector is about 2 m. The continuous and the dashed line represent the Fraunhofer fringes measured through the cylindrical Be window (*i.e.* 4 mm total thickness) and the kapton windows (250 µm of thickness), respectively. The clear signal measured through the kapton is deteriorated in the case of the beryllium. Therefore, for experiments using a coherent X-ray beam, the Be window is replaced by a stainless steel flange with four kapton windows at right angles, shown schematically in the inset of Fig. 2. The 125 µm kapton windows, easily replaceable, are pressed against the chamber by flanges, and viton O-rings are used to seal the vacuum. The angular aperture of each window is 10° in the horizontal plane and 5°
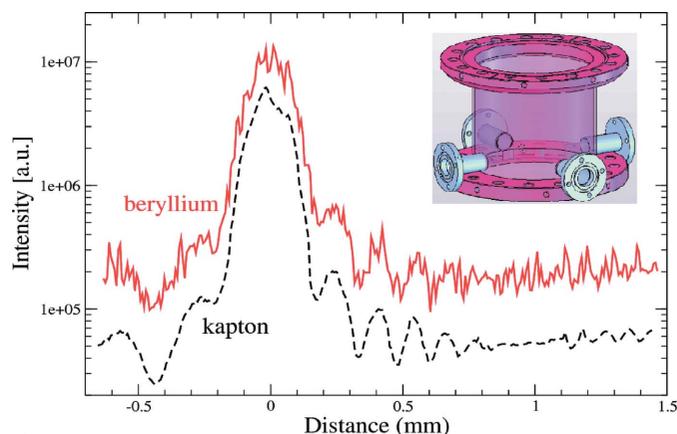
Figure 2
Diffraction from a pair of slits measured through 4 mm of unpolished Be (continuous line) and 250 µm of kapton (dashed line). The curves are vertically shifted for clarity. Note that the asymmetry of the Fraunhofer pattern is due to the longitudinal offset of the slit blades (see Le Bolloc'h *et al.*, 2002). The kapton window preserves the wavefront of the coherent X-ray beam, while spurious speckles are produced by the Be window. Inset: design of the flange with kapton windows.

in the vertical, which allows for GISAXS measurements. The base pressure of the chamber in this configuration is ~1 × 10^{-6} mbar.
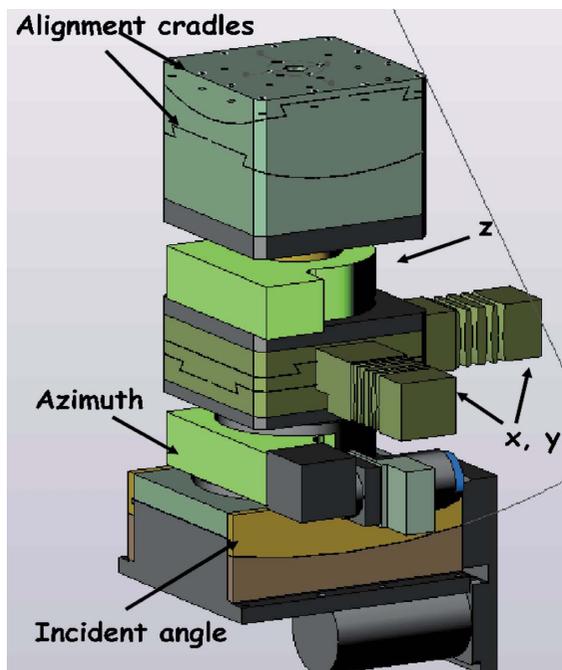
3. Use on diffractometer

The heavy-load 4 + 2-circle diffractometer on beamline ID01 at the European Synchrotron Radiation Facility (ESRF) allows for scattering experiments both in the vertical or horizontal scattering planes. In its standard configuration, which includes a Eulerian cradle, the 2θ, θ, χ and φ circles form a conventional four-circle diffractometer for vertical plane scattering geometry (*cf.* lower panel of Fig. 3). Two additional arcs, μ and γ, rotate, respectively, the sample and the detector arm around the vertical axis and are used for scattering in the horizontal plane.[4]

For *in situ* X-ray scattering measurements, a heavy-duty sample stage suitable for *z*-axis scattering geometry (Bloch, 1985) is mounted at the centre of the ID01 diffractometer, instead of the Eulerian cradle (*cf.* Fig. 3), to hold the chamber. It allows the use of heavy and/or large sample environments such as a cryostat, furnace, vacuum chamber, multi-sample holder *etc.* It has been designed and produced in a collaboration between ID01 at ESRF and the company Huber (Rimsting, Germany), and is commercially available. It can hold weights up to 120 kg. Fig. 3 shows the three translations that move the chamber along the incident X-ray beam (x) and perpendicular to it in the horizontal (y) and vertical plane (z) with submicrometre precision. Two perpendicular tilt angles with 0.001° precision (indicated as *Alignment cradles* in the figure) allow the chamber adjustment. These are used to compensate the tilt of the sample surface in its interior, in order to preserve the optimal scattering geometry for surface-sensitive studies. The azimuthal angle allows a rotation in the

Figure 4
Scheme of the 'vertical sample stage'. The direction of the X-ray beam (x) of the sample rotation axis (y) and the rotation angle (Φ) are indicated.

all different configurations works in a pseudo six-circle mode. All the described motors, as well as the Eulerian cradle, are implemented for the use of the standard HKL-mode of *SPEC*[5]
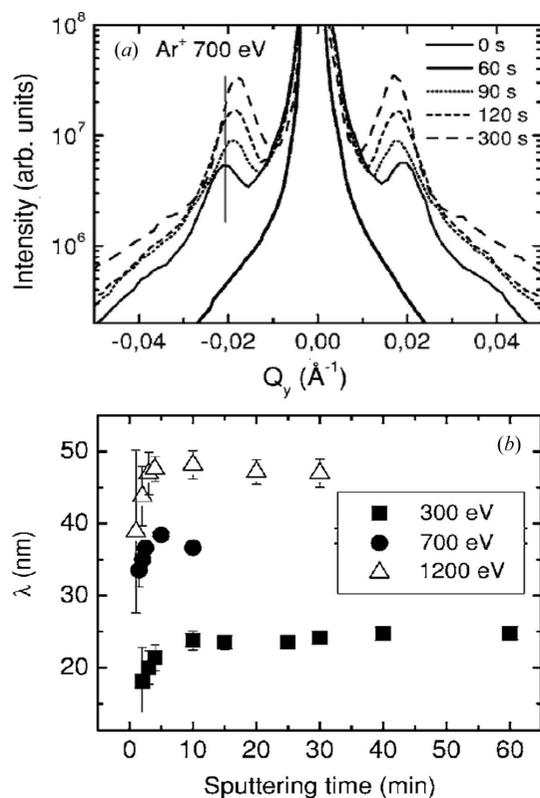
4. Experimental examples

4.1. Nanostructuration of surfaces by IBS

For the study of the kinetics of the nanostructuration process during IBS, we characterize *in situ* the surface morphology, crystalline structure and correlation of nano-structures (dot or ripples) using a combination of different X-ray scattering techniques such as GID, GISAXS and reflectivity. The IBS parameters for the production of surface nanostructures are optimized off-line, prior to the X-ray experiment. During the *in situ* measurements, the input and output values for substrate temperature, and ion beam para-meters (current, acceleration voltage, energy) are handled *via* an interface software controlled by *SPEC*. This allows remote control of the experiment and the synchronization between the nanopatterning process and X-ray measurements.

One example of such an *in situ* experiment is the study of the formation and evolution of dot patterns on GaSb surfaces during Ar^+ IBS at normal incidence. Fig. 5 illustrates the results obtained for different ion energies (Plantevin *et al.*, 2007). The GISAXS profiles measured at different times during the sputtering process show correlation peaks that correspond to the lateral ordering of the dot pattern. The variation of their position in time can be directly related to the variation of the mean inter-dot distance λ during the IBS process (*cf.* Fig. 5b). This has been found to follow the theo-

Figure 3
Top: schematics of the heavy-duty sample stage on the diffractometer of ID01 and its degrees of freedom; the translation and rotation stages are highlighted. Bottom: ID01 diffractometer with z-axis geometry config-uration and Eulerian cradle out.

$360°$ range. The tilt angle at the bottom of the stage inclines the whole tower in a range $\pm 5°$ along the direction of the incident beam, and is used in grazing-incidence experiments. It keeps the X-ray incident angle constant while rotating the sample around its azimuth.

The functionality of this sample stage can be completed using a vertical sample goniometer (*cf.* Fig. 4) that provides a rotation of the sample around a horizontal axis y perpendi-cular to the incident X-ray beam, and a translation with micrometre precision along its rotation axis. This unit is used for coplanar diffraction at large Bragg angles, or for grazing-incidence diffraction in vertical geometry for small sample environments. It can be mounted and unmounted easily and reproducibly, depending on the need. The diffractometer in

[5] *SPEC* scientific software, http://www.certif.com/spec_manual/.

Figure 5
In situ GISAXS measurements showing the temporal evolution of the nanodot pattern created on GaSb(001) surfaces by Ar^+ IBS, using an Ar^+ partial pressure of $\sim 10^{-3}$ mbar, and an ion current density at the sample of $\sim 100 \, \mu A \, cm^{-2}$. (*a*) GISAXS scans at different times during 700 eV Ar^+ IBS. Q_y is the component of the momentum transfer parallel to the sample surface and perpendicular to the impinging X-ray beam. (*b*) Time evolution of the lateral periodicity λ of the patterns for different Ar^+ energies. (From Plantevin *et al.*, 2007.)

retical predictions. More details can be found in Plantevin *et al.* (2007).

4.2. GID studies of oxide surfaces and metal/oxide interfaces

For the characterization and preparation of various thin films and surfaces, including metals on semiconductors, such as silicates (C. Mocuta, unpublished), oxides on metals (Stanescu *et al.*, 2008) and metals on oxides (Bezencenet *et al.*, 2008), the chamber is used under UHV conditions. In addition to *in situ* growth studies, the chamber is suitable for the preparation and characterization of the initial surfaces (including surface reconstruction) before deposition. As an example, we show here the investigation of α-Fe_2O_3(0001) (hematite) films on Pt(111) (Barbier *et al.*, 2007). The samples were grown *ex situ* and transferred in air. The hematite surface had been regenerated inside the chamber by a 30 min outgas at 600 K in 10^{-5} mbar oxygen partial pressure. GID measurements have revealed a dislocation network at the interface between a 20 nm-thick hematite film and the Pt(111) substrate (*cf.* Fig. 6). The real-space distance of this network is found to be ~ 51 Å, in good agreement with the coincidence network expected at the α-Fe_2O_3(0001)/Pt(111) interface. More details can be found in Barbier *et al.* (2007).
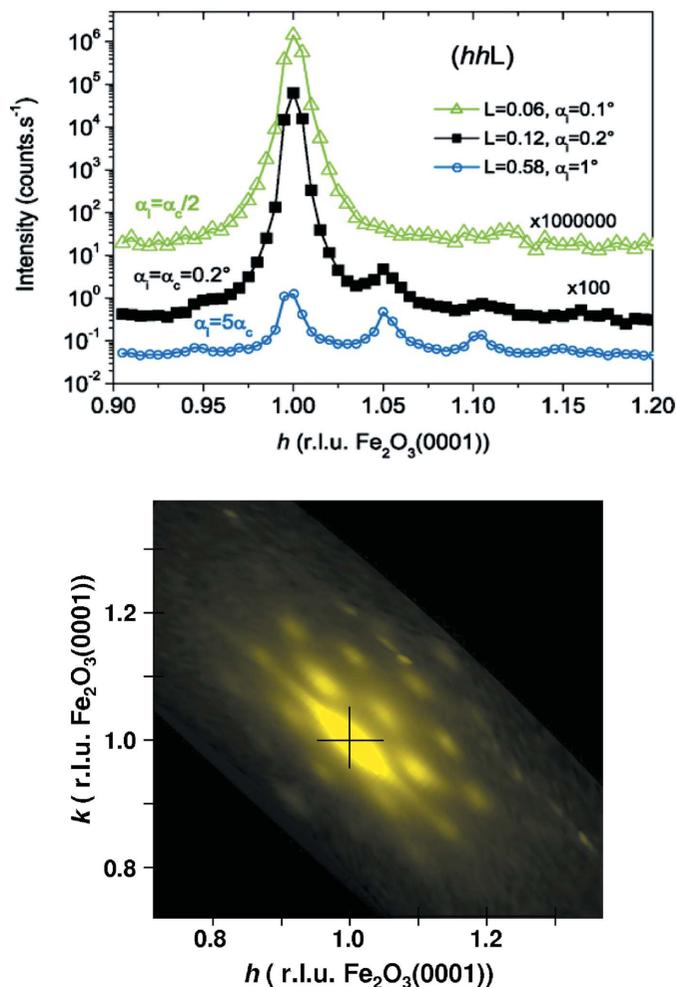
Figure 6
Dislocation network on a 20 nm-thick α-Fe_2O_3(0001) film deposited on Pt(111). Top: (*hh*L) scans as a function the incidence angle. The coordinates are expressed in reciprocal lattice units (r.l.u.) of Fe_2O_3. Emergence is kept equal to incidence. The curves are shifted for clarity. Bottom: reciprocal space map around the (110) peak of α-Fe_2O_3(0001), showing a two-dimensional ordered dislocation network around the hematite Bragg peak (marked by the cross). (From Barbier *et al.*, 2007.)

5. Conclusions

We have presented a portable vacuum chamber, designed for real-time X-ray scattering studies of nanopatterning of semiconductor surfaces by ion beam erosion. Optimized for working in a middle-pressure regime, also with the use of a coherent X-ray beam, it is also adaptable to UHV conditions. Its compact design and its modularity are highlighted. These characteristics make it a very versatile piece of equipment, useful for *in situ* X-ray scattering studies of various systems under different conditions.

References

Ackermann, M. D., Pedersen, T. M., Hendriksen, B. L. M., Robach, O., Bobaru, S. C., Popa, I., Quiros, C., Kim, H., Hammer, B., Ferrer, S. & Frenken, J. W. M. (2005). *Phys. Rev. Lett.* **95**, 255505.

Barbier, A., Bezencenet, O., Mocuta, C., Moussy, J.-B., Magnan, H., Jedrecy, N., Guittet, M.-J. & Gautier-Soyer, M. (2007). *Mater. Sci. Eng. B*, **144**, 19–22.

Bernard, P., Peters, K., Alvarez, J. & Ferrer, S. (1999). *Rev. Sci. Instrum.* **70**, 1478–1480.

Bezencenet, O. *et al.* (2008). To be published.

Bloch, J. M. (1985). *J. Appl. Cryst.* **18**, 33–36.

Carbone, D., Alija, A., Plantevin, O., Gago, R., Facsko, S. & Metzger, T. H. (2008). *Nanotechnology*, **19**, 035304.

Facsko, S., Dekorsy, T., Koerdt, C., Trappe, C., Kurz, H., Vogt, A. & Hartnagel, H. L. (1999). *Science*, **285**, 1551–1553.

Gago, R., Vazquez, L., Cuerno, R., Varela, M., Ballesteros, C. & Albella, J. M. (2001). *Appl. Phys. Lett.* **78**, 3316.

Joumard, I., Torrelles, X., Lee, T.-L., Bikondoa, O., Rius, J. & Zegenhagen, J. (2006). *Phys. Rev. B*, **74**, 205411.

Le Bolloc'h, D., Livet, F., Bley, F., Schulli, T., Veron, M. & Metzger, T. H. (2002). *J. Synchrotron Rad.* **9**, 258–265.

Nicklin, C. L., Taylor, J. S. G., Jones, N., Steadman, P. & Norris, C. (1998). *J. Synchrotron Rad.* **5**, 890–892.

Pietsch, U., Holy, V. & Baumbach, T. (2004). *High-Resolution X-ray Scattering: From Thin Films to Lateral Nanostructures.* New York: Springer Verlag.

Plantevin, O., Gago, R., Vázquez, L., Biermanns, A. & Metzger, T. H. (2007). *Appl. Phys. Lett.* **91**, 113105.

Schmidbauer, M. (2004). *X-ray Diffuse Scattering from Self-Organized Mesoscopic Semiconductor Structures.* Berlin/Heidelberg: Springer Verlag.

Stanescu, S. *et al.* (2008). To be published.

Stangl, J., Roch, T., Holý, V., Pinczolits, M., Springholtz, G., Bauer, G., Kegel, I., Metzger, T. H., Zhu, J. & Brunner, K. (2000). *J. Vac. Sci. Technol. B*, **18**, 2187.

Valbusa, U., Boragno, C. & Buatier de Mongeot, F. (2002). *J. Phys. Condens. Matter*, **14**, 8153.

Valvidares, S. M., Schroeder, T., Robach, O., Quirós, C., Lee, T.-L. & Ferrer, S. (2004). *Phys. Rev. B*, **70**, 224413.

Ziberi, B., Frost, F., Hoeche, T. & Rauschenbach, B. (2005). *Phys. Rev. B*, **72**, 235310.